Diagnostic Value of Pericholedochal Hypointense Ring Sign in MRI T2W Images in Cases of Pancreatic Ductal Adenocarcinoma

Ozlem Akinci, Ercan Inci, Mustafa Orhan Nalbant, Ozkan Oner and Elif Hocaoglu

Department of Radiology, Bakirkoy Dr Sadi Konuk Training and Research Hospital, Istanbul, Turkiye

ABSTRACT

Objective: To determine the value of hypointense pericholedocal ring sign in magnetic resonance imaging (MRI) T2W sequence images in the diagnosis of pancreatic ductal adenocarcinoma (PDA).

Study Design: Retrospective observational study.

Place and Duration of the Study: Department of Radiology, Bakirkoy Dr Sadi Konuk Training and Research Hospital, Istanbul, Turkiye, from January 2016 and March 2022.

Methodology: Retrospective analysis of MRI scans was performed on 70 patients with postoperative histopathological confirmation of a diagnosis of periampullary cancer. The patients' demographic information, the results of their histopathological examinations, and the findings of their MRIs were recorded. The results of the MRI were statistically analysed and compared between the PDA and the non-PDA groups.

Results: The study included 43 (61.4%) male and 27 (38.5%) female patients, with a mean age of 62.2 ± 8.4 years. The means of Wirsung diameter and tumour diameter were significantly higher in PDA group ($p = 0.034$, $p = 0.010$, respectively). A progressive contrast enhancement pattern of 95.3% was observed in PDA group, while 40.7% rapid contrast enhancement pattern was observed in the non-PDA group. Hypointense pericholedochal ring sign, observed in T2W sequences, was detected in 74.2% ($n = 32$) of the PDA group and 11.1% ($n = 3$) of the non-PDA group, and the findings were statistically significant ($p <0.001$).

Conclusion: Hypointense pericholedochal ring sign in axial T2W sequences in periampullary tumours is a complementary MRI finding in the distinction between the PDA and the non-PDA groups.

Key Words: *Magnetic resonance imaging, Pancreatic ductal adenocarcinoma, Periampullary tumours, Pericholedochal ring sign.*

How to cite this article: Akinci O, Inci E, Nalbant MO, Oner O, Hocaoglu E. Diagnostic Value of Pericholedochal Hypointense Ring Sign in MRI T2W Images in Cases of Pancreatic Ductal Adenocarcinoma. *J Coll Physicians Surg Pak* 2024; **34(09)**:1101-1106.

INTRODUCTION

Periampullary cancers include carcinomas originating from four different anatomical regions adjacent to the major duodenal papilla. The tumour groups are the pancreatic head tumours, common bile duct (CBD) tumours, duodenal, and ampullary tumours. These four cancer groups show different molecular and biological characteristics, and each has a different prognosis.[1] Previous studies have shown that overall survival (OS) is highest in ampullary and duodenal cancers, medium in CBD tumours, and lowest in pancreatic cancer.[2-4] The most frequent malignant tumour of the pancreas is pancreatic ductal adenocarcinoma (PDA). PDA is the seventh most prevalent cancer-related cause of mortality worldwide.

Correspondence to: Dr. Ozlem Akinci, Department of Radiology, Bakirkoy Dr Sadi Konuk Training and Research Hospital, Istanbul, Turkiye
E-mail: dr.ozlemgungor@yahoo.com

Received: May 20, 2023; Revised: January 07, 2024; Accepted: April 28, 2024
DOI: https://doi.org/10.29271/jcpsp.2024.09.1101

The mean 5-year survival rate for this highly aggressive tumour is below 5%.[5] About 20% of patients have access to surgical resection, the only potentially curative treatment option.

Preoperative imaging and even postoperative histological examination can have difficulty in pinpointing the precise location of anatomical origin in these tumours because of their close proximity to one another and the complexity of the regional anatomy. This makes it difficult to determine the exact location of the anatomical origin.[1] When compared to other periampullary tumours, PDAs have a poor prognosis and a variety of adjuvant treatment options. For this reason, it is essential to make this distinction. A diagnosis of PDA prior to surgery enables efficient planning of neoadjuvant and adjuvant treatment, and it also has the potential to reduce the risk of local recurrence as well as the risk of distant metastases as the disease progresses. As a result of recent developments, magnetic resonance imaging (MRI) is now playing an increasingly important role in the diagnosis of diseases affecting the pancreas and biliary system.[6] Prior to surgery, it is necessary to discover new therapeutic and prognostic predictive markers in order to make the most of the treatment modalities available to patients with periampullary cancers. In order to better assess the prognosis of

individual patients, many researchers have attempted to distinguish between these cancers using various imaging modalities. Imaging techniques such as computed tomography (CT) and MRI are typically utilised in order to make a diagnosis of cancer in the periampullary region. It has been demonstrated that MR imaging with MR cholangiopancreatography (MRCP) is more accurate than CT imaging in distinguishing benign from malignant periampullary lesions. This is because MRCP offers more precise details about the pancreatic and biliary duct anatomy than the CT imaging does.[7] It has been hypothesised that MRI has the ability to forecast disease-free survival as well as OS in PDA patients who have undergone curative resection.[8]

There is currently no specific imaging guide for the differential diagnosis of periampullary cancers, despite the advancements in imaging techniques.[9] When trying to determine where periampullary cancers originate from, the position of the tumour's central mass and whether or not there is dilatation of the pancreatic duct and the CBD are two crucial factors to take into account. It is possible for periampullary masses other than PDA to infiltrate the pancreatic head, which would result in dilatation of both the CBD and the pancreatic duct. This would indicate that the pancreatic head has been invaded by the masses. On an MRI, the PDA appears as a hypointense mass and is the portion of the periampullary mass that grows to the greatest size. On the other hand, PDA is characterised by a high cellularity despite its relatively low levels of fibrotic stroma. As a consequence of this, it shows up on MR or CT scans as a mass that is isointense or isoattenuating.[2,10] It is possible that PDA will cause an obstruction in the intrapancreatic bile duct, which will show up on T2W sequences as a hypointense ring sign around the CBD.[1]

Preoperative diagnosis is crucial because there are various adjuvant treatment options for PDA, which has the worst prognosis of all periampullary masses. This study aimed to determine the diagnostic utility of the hypointense ring sign around the CBD seen in MRI-T2W sequences for PDA among the periampullary tumours.

METHODOLOGY

This retrospective analysis comprised 70 patients who underwent surgery and preoperative MRI and were histopathologically diagnosed with periampullary carcinoma between January 2016 and March 2022 in Bakirkoy Dr Sadi Konuk Training and Research Hospital, Istanbul, Turkiye. The study received approval from the Hospital's Ethics Committee (Approval Number: 09.05.2022/2022-09-20). Informed consent was obtained from all patients. The study was completed in 4 months.

Cancers of the periampullary region were previously classified as pancreatic adenocarcinomas, tumours of the CBD, tumours of the ampulla of Vater, and tumours of the periampullary region of the duodenum. Patients without preoperative MRI and patients who received neoadjuvant therapy before MRI were excluded from the study. In addition, cases of polypoid-type distal CBD cancer were omitted from the analysis, as these cases can be easily distinguished from other periampullary tumours. The study excluded 34 patients who had not undergone an MRI or MRCP examination, 10 patients who had undergone preoperative surgical procedures, in addition to six patients whose image quality was unsuitable for analysis due to the presence of motion artefacts. Time from MRI to surgery ranged from 2 to 22 days (average = 13 days).

Demographic data, histopathological results, and MRI findings of the patients were obtained from the hospital archive system. The diameter (mm) and the distal shape of CBD, the tumour diameter (mm), the contrast pattern, and signal intensity of the lesion in T1W and T2W sequences were evaluated on the MRI in comparison to the duodenum and pancreas. The CBD, Wirsung, and tumour diameters were measured on MRI T2AW axial sections with reference to the widest diameter. The enhancement pattern can be broken down into two distinct subtypes: Either high enhancement, which reaches its highest point during the arterial or venous phase, or progressive enhancement, which reaches its highest point during the equilibrium or delayed phase. The hypointense ring sign was defined as a dark ring around the CBD in MRI T2W sequences (Figure 1 and 2). All cases were retrospectively and separately evaluated by two radiologists with experience of 7 and 10 years in abdominal MRI. All patients were known to have periampullary cancers, although the exact histological diagnosis was unknown to the observers. The patients were divided into two groups: PDA and non-PDA (patients with a pathological diagnosis of CBD cancer, ampullary adenocarcinoma, and duodenal cancers). There were 43 cases in the PDA group and 27 cases in the non-PDA group. MRI findings between the PDA and non-PDA groups were statistically analysed to make comparisons.

For MRI scan, a 3.0 T MR system (Verio; Siemens Medical Solutions, Erlagen, Germany) and a 16-channel phased array surface coil were used. Thin-section turbo spin-echo (TSE) T2-weighted images were acquired in the sagittal, transverse, and coronal planes during the imaging sequences. Each slice had a thickness of 3 mm and lacked an intersection gap. The repetition time (TR) and echo time (TE) were set at 5,800 ms and 100 ms, respectively. Patients were instructed to abstain from food for at least four hours prior to their MRI appointments. The fast spin-echo (SE) technique was used to acquire thick-slab single-section T2-weighted MRCP images in at least six different planes while the patient was holding their breath. These planes included the sagittal, coronal, and coronal oblique planes. For the purpose of three-dimensional (3D) MRCP, a 3D fast-recovery turbo SE sequence was performed. T1-weighted 3D turbo-field-echo sequences were used to obtain unenhanced, arterial-phase (20 - 35s), portal-phase (60s), 3 minutes late-phase, and 20 minutes hepatobiliary phase images for gadoxetic acid-enhanced imaging. These images were acquired using a T1-weighted 3D turbo-field. A 20 ml saline wash was conducted after the contrast agent was administered intravenously at a rate of 1 ml/s at a dose of 0.025 mmol/kg. This was done using a power injector. After the data had been transferred to a workstation, 3D MRCP pictures using maximum intensity projection were rebuilt.

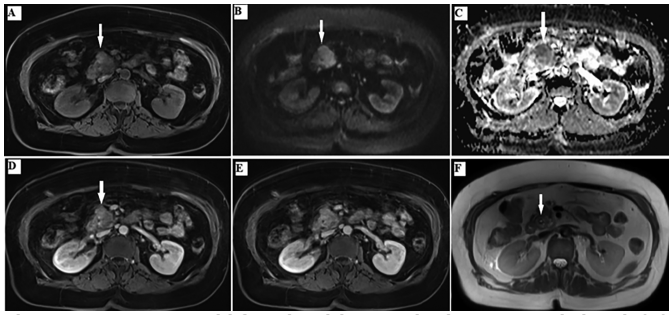

Figure 1: A 60-year-old female with PDAC in the pancreatic head. (A) Unenhanced T1-weighed image of the lesion is iso-hypointense, (B) The diffusion-weighted image shows hyperintensity, and the apparent diffusion coefficient image, (C) shows hypointensity consistent with diffusion restriction (white arrows), (D-E) gadoxetic acid-enhanced portal-venous and delayed phase show an ill-defined hypointense mass (arrows) in the pancreatic head which shows increasing contrast towards the late phase, (F) T2W image shows a small thin dark ring (pericholedochal hypointense ring sign), (arrow) in the centre of the mildly hyperintense CBD.

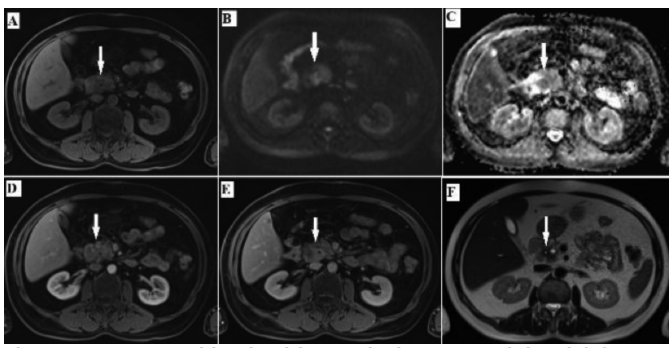

Figure 2: A 55-year-old male with PDAC in the pancreatic head. (A) Unenhanced T1-weighed image of the lesion is iso-hypointense, (B) The diffusion-weighted image shows hyperintensity, and the apparent diffusion coefficient image, (C) shows hypointensity, (D-E) gadoxetic acid-enhanced portal-venous and delayed phase show an ill-defined hypointense mass (arrows) in the pancreatic head which shows increasing contrast towards the late phase, (F) T2W image shows a small thin dark ring (pericholedochal hypointense ring sign), in the centre of the mildly hyperintense CBD.

The level of agreement between the two observers was determined with the help of the interclass correlation coefficient (ICC) or Cohen's Kappa statistic. The Kappa values and ICCs for all parameters, with the exception of T1 and T2 signal intensity in comparison to duodenum and pancreas (values of Kappa varying from 0.72 to 0.82), exceeded to 0.85, which indicates that there was an almost perfect agreement between the parameters (Table I).

All of the statistical work was done by SPSS version 25.0. In order to determine whether or not the variables followed a normal distribution, the histogram graphics and the Kolmogorov-Smirnov test were utilised. The values for the mean, the standard deviation, the median, and the interquartile range were utilised in the presentation of descriptive analyses. Categorical variables were given as numbers (n) and percentages (%). The Pearson's Chi-squared test was utilised in order to make comparisons between categorical variables. The Mann-Whitney U test was used to analyse non-parametric variables compared between the two groups. The results were deemed statistically significant if they had a p-value of <0.05.

Table I: MRI image features Kappa values for lesions measured by two observers.

	Weighted Kappa	Level of agreement
Hypointense ring sign	0.94	Almost perfect
The shape of the distal edge of the CBD	0.85	Almost perfect
Symmetry of the distal lumen of the CBD	0.87	Almost perfect
The shape of the narrowing of the distal end of the CBD	0.86	Almost perfect
Oval filling defect in the distal part of the CBD	0.92	Almost perfect
Pattern of contrast enhancemet	0.94	Almost perfect
Signal intensity - duodenum T1W	0.72	Substantial
Signal intensity - pancreas T1W	0.73	Substantial
Signal intensity - duodenum T2W	0.80	Almost perfect
Signal intensity - pancreas T2W	0.82	Almost perfect

RESULTS

Forty-three (61.4%) patients in the study were males and 27 (38.5%) were females, and the mean age was 62.2 ± 8.4 years. The mean diameters of the tumour and CBD in all cases were 24.7 ± 9.4 and 11.3 ± 4.5 mm, respectively. The contrast enhancement pattern was progressive in 74.3% of the cases.

The mean age and the mean CBD diameter of the non-PDA group were higher than those of the PDA group ($p = 0.044$ and $p = 0.033$, respectively, Table II). The means of Wirsung diameter and tumour diameter were higher in PDA group ($p = 0.034$ and $p = 0.010$, respectively, Table II).

The signal intensity in T1W sequences did not differ significantly between the PDA and non-PDA groups based on whether the CBD had a regular or irregular distal edge, a symmetrical or asymmetrical distal lumen, a sudden or pointed termination at the distal end, and whether the lesion was located in the duodenum or pancreatic parenchyma ($p > 0.05$, Table II). A progressive contrast enhancement pattern of 95.3% was observed in the PDA group, while a 40.7% rapid contrast enhancement pattern was observed in the non-PDA group ($p < 0.001$). The "oval filling defect in the distal CBD" (16.3%) was significantly lower in the PDA group ($p < 0.001$).

Hypointense ring signs were observed around the CBD in T2W sequences in 74.2% (n=32) of the PDA group and 11.1% (n=3) of the non-PDA group, and the findings were statistically significant ($p < 0.001$, Table III). The incidence of hypointense appearance of the lesion in T2W sequences compared to the duodenum and pancreas was significantly higher in the PDA group ($p=0.010$; $p=0.027$, respectively).

DISCUSSION

Considering the poor prognosis and different adjuvant treatment options, it is important to distinguish PDAs from other periampullary tumours. The combined use of conventional MRI and MRCP is superior to CT in the differential diagnosis of periampullary masses.[11]

Table II: Comparison of demographic data, CBD characteristics, Wirsung, and tumour diameters of pancreatic duct adenocarcinomas (PDAs) and non-PDA groups.

		PDA Group n:43	Non-PDA Group n:27	Total n:70	p-value
Age*		60 (54 - 69)	65 (61 - 68)	63 (46 - 77)	0.044[a]
Gender**	Male	26 (37.1)	17 (24.3)	43 (61.4)	0.834[b]
	Female	17 (24.3)	10 (14.3)	27 (38.6)	
The shape of the distal edge of the CBD**	Regular	22 (31.4)	16 (22.8)	38 (54.3)	0.508[b]
	Irregular	21 (30.0)	11 (15.7)	32 (45.7)	
Symmetry of the distal lumen of the CBD**	Symmetric	20 (28.6)	11 (15.7)	31 (44.3)	0.636[b]
	Asymmetric	23 (32.8)	16 (22.8)	39 (55.7)	
The shape of the narrowing of the distal end of the CBD**	Tapering	17 (24.3)	9 (12.8)	26 (37.1)	0.601[b]
	Abrupt termination	26 (37.1)	18 (25.7)	44 (62.8)	
Oval filling defect in the distal part of the CBD**	No	36 (51.4)	10 (14.3)	46 (65.7)	<0.001[b]
	Yes	7 (10.0)	17 (24.3)	24 (34.3)	
Diameter of CBD (mm)*		10 (6.9 - 13.8)	12.5 (10.5 - 16)	12 (3 - 23)	0.033[a]
Diameter of wirsung (mm)*		5.5 (3.4 - 7.5)	3.5 (3 - 6)	4.5 (1.5 - 11)	0.034[a]
Diameter of tumour (mm)*		25 (21 - 31)	22 (12 - 26)	24 (10 - 56)	0.010[a]

*[*]Median (IQR), **n (%), [a]Mann-Whitney U Test, [b]Chi-square test.*

Table III: Comparison of MRI findings and contrast enhancement patterns of pancreatic duct adenocarcinomas (PDAs) and non-PDA groups.

		PDA Group n:43 (%)	Non-PDA Group n:27 (%)	Total n: 70 (%)	p-value
Hypointense ring sign		32 (45.7)	3 (4.3)	35 (50)	<0.001
Pattern of contrast enhancemet	Rapid	2 (2.8)	16 (22.8)	18 (25.7)	<0.001
	Progressive	41 (58.6)	11 (15.7)	52 (74.3)	
Signal intensity - duodenum T1W*	Hyperintense	3 (4.3)	0 (0.0)	3 (4.3)	0.351
	Hypointense	19 (27.1)	14 (20.0)	33 (47.1)	
	Isointense	21 (30.0)	13 (18.6)	34 (48.6)	
Signal intensity - pancreas T1W*	Hyperintense	3 (4.3)	0 (0.0)	3 (4.3)	0.141
	Hypointense	23 (32.8)	20 (28.6)	43 (61.4)	
	Isointense	17 (24.3)	7 (10.0)	24 (34.3)	
Signal intensity - duodenum T2W**	Hyperintense	14 (20.0)	13 (18.6)	27 (38.6)	0.010
	Hypointense	15 (21.4)	1 (1.4)	16 (22)	
	Isointense	14 (20.0)	13 (18.6)	27 (38.6)	
Signal intensity - pancreas T2W**	Hyperintense	17 (24.3)	13 (18.6)	30 (42.8)	0.027
	Hypointense	17 (24.3)	3 (4.3)	20 (28.6)	
	Isointense	9 (12.8)	11 (15.7)	20 (28.6)	

*Chi-square test. *Signal intensity of the lesion relative to the duodenum / pancreas T1W sequences. **Signal intensity of the lesion relative to the duodenum / pancreas T2W sequences.*

The joint evaluation of the MRCP, T1W, and T2W gadolinium post-contrast T1W MRI series is of great importance in the differential diagnosis of periampullary masses. Periampullary tumours present in different ways due to their location. When they cause obstruction at the level of the major papilla, ampullary carcinomas typically take the form of a small tumour. On the other hand, pancreatic carcinomas frequently take the form of large masses, and bile duct carcinomas frequently take the form of thickening of the ductal wall.

It is possible for the signal intensity of periampullary cancers on T1W and T2W MR images to vary in comparison to the signal intensity of the pancreas.[12,13] When the signal intensities of the duodenum and the pancreas were compared, this research revealed that there was no discernible difference between the two.

The increasing contrast enhancement pattern towards the late phase in tumours with abundant fibrous stroma has been previously shown in many studies in the literature, and PDA lesions contain dense fibrous tissue and desmoplastic stroma.[14,15] Similar to the literature, when the MRI enhancement patterns of the PDA and non-PDA groups were compared in this study, progressive enhancement patterns were observed in the majority of the PDA group (p <0.001).[9] Additionally, the contrast uptake in the PDA group showed a peak in the late phase of this study.

PDA is observed as hypointense in the T1W and T2W series due to its intense fibrous stromal content.[16] When the PDA and non-PDA group lesions were compared in T2W sequences, the present study found that PDA lesions were significantly more hypointense than the pancreas and duodenum parenchyma (p <0.001). On the other hand, the results of this research showed that there was no discernible difference in the frequency of the hypointense appearance of the lesion in T1W sequences when compared to the pancreas and the duodenum.

Because of their unique biological behaviour, desmoplastic reactions, and tumour localisation, periampullary carcinomas are responsible for alterations in the CBD.[1] The distal end of CBD, as well as its abruptness and pointiness, did not differ significantly between the PDA and non-PDA groups in this study. It was found that the frequency of oval filling defects in the distal CBD was significantly higher in the non-PDA group compared to the PDA group. This finding is in line with the research that has been done previously.

The hypointense pericholedochal ring sign was observed in T2W axial sections in this study, and it was positive in 75% of the patients in the PDA group and in 11% of the patients in the non-PDA group. Furthermore, the prevalence of this sign was significantly greater in the PDA group than the non-PDA group ($p < 0.001$). PDA is observed as a hard, whitish mass in tumour specimens due to its abundant fibrous stroma. Hypointense ring images are formed in T2W sequences around CBD, surrounded and compressed by a mass rich in fibrous tissue. In contrast to PDA carcinomas, CBD cancers are characterised by a thickening of the wall of CBD as well as a slightly hyperintense appearance around the CBD in T2W sequences in comparison to the pancreatic parenchyma that surrounds the tumour.[1] There is the extremely low frequency of the T2W hypointense choledochal ring sign in CBD cancer. The centrifugal tumour growth pattern of CBD cancer, which does not include the intraductal-growing polypoid type, may be able to explain the exceptionally low frequency of the T2W hypointense choledochal ring sign that is seen in patients with CBD cancer. This is in contrast to the centripetal pattern of bile duct narrowing that occurs in PDA as a result of tumour engulfment. In PDA, the bile duct narrows in a centripetal pattern. Several studies in the literature have shown that PDAs that are isointense with the pancreatic parenchyma can easily be overlooked on contrast-enhanced CT and MRI.[10,17] The T2 dark choledochal ring sign is a potential indicator of PDAs for these tumours.

Cha *et al*. argued that the use of the hypointense ring sign in lesions with large diameters would not be suitable, as the hypointense ring sign was observed in two non-PDA cases with 3.5 and 4 cm diameters.[1] Similarly, in the present study, the tumour diameter was between 3.0 and 3.5 cm in two of the three patients with hypointense ring signs around the CBD in the non-PDA group.

In this study, the pericholedochal hypointense ring sign was investigated in a similar way to the study of Cha *et al*. In addition, many MRI parameters that can be used to distinguish between PDA and non-PDA were examined.

The current study had a number of important limitations. First, because the present study was conducted using a retrospective design, it is inevitable that there was some selection bias despite the use of strict inclusion criteria. Patients who had reached an advanced stage of the disease and were unable to undergo surgery were not included in the current study because the population included tumours that had been resected surgically. Additionally, considering that the hypointense ring sign can be observed in non-PDA lesions as the tumour diameter increases, not performing a comparison within the sub-groups by dividing tumour diameters into certain groups can be considered a limitation. In addition, this study was conducted at a single centre; consequently, multicentric studies involving a greater number of participants are required to verify the results of this investigation.

CONCLUSION

The presence of a hypointense pericholedochal ring sign in axial T2W sequences in periampullary tumours can be used as a complementary MRI finding in the distinction between the PDA and the non-PDA tumours.

ETHICAL APPROVAL:
The study received approval from the Hospital's Ethics Committee (Approval Number: 09.05.2022/2022-09-20).

PATIENTS' CONSENT:
Informed consent was obtained from all patients.

COMPETING INTEREST:
The authors declared no conflict of interest.

AUTHORS' CONTRIBUTION:
OA, MON, OO: Study design, conception, patient selection, and manuscript writing.
EI, EH: Critical revision for important intellectual content and providing clinical expertise.
All authors approved the final version of the manuscript to be published.

REFERENCES

1. Cha D I, Kim YK, Choi SY, Lim SH, Choi D, Lee WJ. Pancreatic ductal adenocarcinoma: Prevalence and diagnostic value of dark choledochal ring sign on T2-weighted MRI. *Clin Radiol* 2014; **69(4)**:416-23. doi: 10.1016/j.crad.2013.11.015.
2. Kim JH, Kim MJ, Chung JJ, Lee WJ, Yoo HS, Lee JT. Differential diagnosis of periampullary carcinomas at MR imaging. *Radiographics* 2002; **22(6)**:1335-52. doi: 10.1148/rg.226025060.
3. Chan C, Herrera MF, de la Garza L, Quintanilla-Martinez L, Vargas-Vorackova F, Richaud-Patin Y, *et al*. Clinical behavior and prognostic factors of periampullary adenocarcinoma. *Ann Surg* 1995; **222(5)**:632-7. doi: 10.1097/00000658-199511000-00005.
4. Carter JT, Grenert JP, Rubenstein L, Stewart L, Way LW . Tumors of the ampulla of vater: Histopathologic classification and predictors of survival. *J Am Coll Surg* 2008; **207(2)**: 210-8. doi: 10.1016/j.jamcollsurg.2008.01.028.
5. Jemal A, Siegel R, Ward E, Hao Y, Xu J, Murray T, *et al.* Cancer statistics, 2008. *CA Cancer J Clin* 2008; **58(2)**: 71-96. doi: 10.3322/CA.2007.0010.
6. Jha P, Yeh BM, Zagoria R, Collisson E, Wang ZJ. The role of MR imaging in pancreatic cancer. *Magn Reson Imaging Clin N Am* 2018; **26(3)**:363-73. doi: 10.1016/j.MRI c.2018.03.004.
7. Park HS, Lee JM, Choi HK, Hong SH, Han JK, Choi B I. Preoperative evaluation of pancreatic cancer: Comparison of gadolinium-enhanced dynamic MRI with MR cholangiopancreatography *versus* MDCT. *J Magn Reson Imaging* 2009; **30(3)**:586-95. doi: 10.1002/jMRI .21889.

8. Lee S, Kim SH, Park HK, Jang KT, Hwang JA, Kim S. Pancreatic ductal adenocarcinoma: Rim enhancement at MR imaging predicts prognosis after curative resection. *Radiology* 2018; **288(2)**:456-66. doi: 10.1148/radiol.2018172331.
9. Bi L, Dong Y, Jing C, Xiu J, Cai S, Huang Z, *et al*. Differentiation of pancreatobiliary-type from intestinal-type periampullary carcinomas using 3.0T MRI. *J Magn Reson Imaging* 2016; **43(4)**:877-86. doi: 10.1002/jMRI .25054.
10. Ishigami K, Yoshimitsu K, Irie H, Tajima T, Asayama Y, Nishie A, *et al*. Diagnostic value of the delayedphase image for iso-attenuating pancreatic carcinomas in the pancreatic parenchymal phase on multidetector computed tomography. *Eur J Radiol* 2009; **69(1)**:139-46. doi: 10.1016/j.ejrad.2007.09.012.
11. Andersson M, Kostic S, Johansson M, Lundell L, Asztely M, Hellstrom M. MRI combined with MR cholangiopancreatography *versus* helical CT in the evaluation of patients with suspected periampullary tumors: A prospective comparative study. *Acta Radiol* 2005; **46(1)**:16-27. doi: 10.1080/02841850510016018.
12. Semelka RC, Kelekis NL, John G, Ascher SM, Burdeny D, Siegelman ES . Ampullary carcinoma: Demonstration by current MR techniques. *J Magn Reson Imaging* 1997; **7(1)**:153-6. doi: 10.1002/jMRI.1880070122.
13. Irie H, Honda H, Shinozaki K, Yoshimitsu K, Aibe H, Nishie A, *et al*. MR imaging of ampullary carcinomas. *J Comput Assist Tomogr* 2002; **26(5)**:711-7. doi: 10.1097/00004728-200209000-00008.
14. Wang Y, Liang Y, Xu H, Zhang X, Mao T, Cui J, *et al*. Single cell analysis of pancreatic ductal adenocarcinoma identifies a novel fibroblast subtype associated with poor prognosis but better immunotherapy response. *Cell Discov* 2021; **7(1)**:36. doi: 10.1038/s41421-021-00271-4.
15. Dougan SK. The pancreatic cancer microenvironment. *Cancer J* 2017; **23(6)**:321-5. doi: 10.1097/PPO.0000000000000288.
16. Chung YE, Kim MJ Park MJ, Choi JY, Kim H, Kim SK, *et al*. Differential features of pancreatobiliary- and intestinal-type ampullary carcinomas at MR imaging. *Radiology* 2010; **257(2)**:384-93. doi: 10.1148/radiol.10100200.
17. Pavan T, Omer J, Banke A. Imaging of pancreatic cancer: An overview. *J Gastrointest Oncol* 2011; **2(3)**:168-74. doi: 10.3978/j.issn.2078-6891.2011.036.